Displacement and Distance Measurement using the Change in Junction Voltage Across a Laser Diode due to the Self-Mixing Effect

Yah Leng Lim[1], K. Bertling[1], Pierre Rio[2], J. R. Tucker[1], A. D. Rakić[1]

[1]School of Information Technology and Electrical Engineering, The University of Queensland, Brisbane, QLD, 4072

[2] Institut de Formation d'Ingenieurs de Paris-Sud, Département Optronique, Université Paris-Sud 11, 91 405 Orsay cedex, France

ABSTRACT

The conventional self-mixing sensing systems employ a detection scheme utilizing the photocurrent from an integrated photodiode. This work reports on an alternative way of implementing a Vertical-Cavity Surface-Emitting Laser (VCSEL) based self-mixing sensor using the laser junction voltage as the source of the self-mixing signal. We show that the same information can be obtained with only minor changes to the extraction circuitry leading to potential cost saving with reductions in component costs and complexity. The theoretical linkage between voltage and photocurrent within the self-mixing model is presented. Experiments using both photo current and voltage detection were carried out and the results obtained show good agreement with the theory. Similar error trends for both detection regimes were observed.

Keywords: VCSEL, self-mixing, voltage sensing, laser range finder, distance measurement, optical feedback.

1. INTRODUCTION

In many self-mixing type displacement and ranging system, the self-mixing effect that occurs within the semiconductor laser diode (LD) is usually monitored using a photodiode [1-5]. This technique has proven to be robust and reliable, but generally requires an additional photodiode in the laser package for measurements, increasing manufacturing costs. An alternative method of monitoring self-mixing within the laser is to measure the junction voltage across the laser itself [6, 7]. Therefore, in this sensing scheme LD is used both as a source of light and the sensing element.

Using LD junction voltage change for sensing provides many advantages over photocurrent sensing method including reduction in component cost as the photodiode is no longer needed in the laser package and significant increase in the signal bandwidth. The bandwidth of the voltage signal depends directly on the modulation bandwidth of the laser diode, which is typically in the gigahertz range. This compares favorably with the bandwidth of the integrated photodiode which is typically in the range or tens of kilohertz as it original intention is only to monitor the DC power level in the laser.

In this paper, we report for the first time on a displacement and ranging system based on the self-mixing effect in a Vertical-Cavity Surface Emitting Laser diode (VCSEL) via measuring the laser junction voltage. In Section 2 we present the theoretical model for a self-mixing VCSEL based sensor with voltage-sensing. Section 3 outlines the application of self-mixing mechanism to displacement and distance measurements. Experimental setup enabling the comparison between the voltage and current sensing schemes is introduced in Section 4 and the results obtained are presented and discussed in Section 5.

2. SELF-MIXING

The self-mixing effect can be observed when a fraction of the light emitted from a laser is injected back into the laser cavity by reflection from an external target. Figure 1 shows a three mirror Fabry-Perot cavity model [5, 8-10], frequently used to describe this phenomenon. M_1 and M_2 represent the two mirrors of the laser cavity with amplitude reflection coefficients r_1 and r_{2s} respectively separated by laser cavity of length L. The target is represented by an external mirror

with reflection coefficient r_{ext}. An internal monitor photodiode integrated into the package of a commercial laser diode is used to observe the optical power fluctuations from the laser with self-mixing.
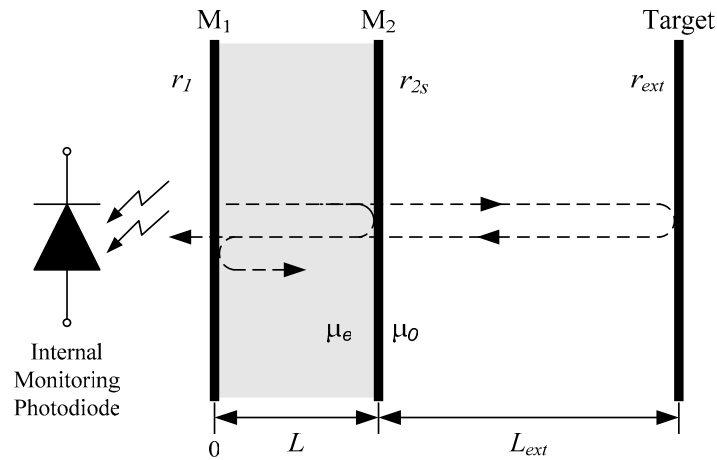

Figure 1: Three-mirror Fabry-Perot cavity model of a semiconductor laser diode with the external reflector

This model can be reduced to the one shown in fig. 2. The second mirror M_2 and the target are combined into a single equivalent mirror with a complex reflection coefficient r_2.
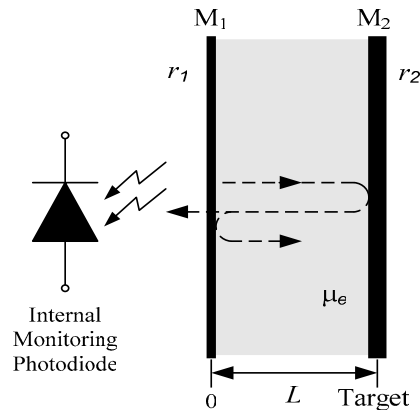

Figure 2: Equivalent Fabry Perot cavity with combined external mirror

The reflection coefficient of this mirror changes with target length L_{ext} and consequently the round-trip propagation time of the external cavity, τ_{ext}. The equivalent mirror reflection coefficient is given by [5, 11, 12],

$$r_2(v) = r_{2s} + (1 - |r_{2s}|^2) r_{ext} \exp(-j2\pi v \tau_{ext}) \ , \tag{1}$$

$$\tau_{ext} = \frac{2L_{ext}}{c} \ ,$$

where,

v	emission frequency of laser with feedback,
τ_{ext}	round trip propagation time in external cavity,
c	speed of light in free space.

Due to the coherence of the emitted light the reflected light will be superimposed in a deterministic way with the light inside the laser cavity depending on the phase shift introduced by the round trip travel to and from the target. This can be interpreted in terms of the equivalent mirror model as a phase change in the reflection coefficient r_2 as indicated in by the second term of eqn (1). This leads to changes in the properties of the light emitted from the laser including the output frequency, the line width, the threshold gain and consequently the output power.

In a Fabry-Perot resonator the round-trip phase shift has to be zero or an integral number of 2π for the lasing condition to be satisfied. Equation (2) [8], relates the change in the laser emission frequency and the excess phase of the cavity of the laser under feedback

$$\Delta\phi_L = 2\pi\tau_{ext}(\nu - \nu_{th}) + C\sin(2\pi\nu\tau_{ext} + \arctan\alpha) \ ,$$ (2)

$$C = \frac{\tau_{ext}}{\tau_L}\kappa_{ext}\sqrt{(1+\alpha^2)} \ ,$$

where,

ν_{th}	laser's natural lasing frequency without feedback,
α	line-width enhancement factor,
$\tau_L = \dfrac{2\mu L}{c}$	round-trip propagation time of the laser cavity,
μ	effective group refractive index,
$\kappa_{ext} = \dfrac{r_{ext}}{r_{2s}}(1 - |r_{2s}|^2)$	coupling coefficient of the external cavity, indicative of the quantity of light being coupled outside of the laser cavity,
C	the feedback coefficient which indicates the amount of light reflected from the external reflector back into the laser cavity,

Using the lasing condition and setting the excess phase $\Delta\phi_L$ to zero one can numerically solve (2) to obtain the emission frequency of laser with feedback ν. Under weak feedback levels (C <1), there is only one solution for the emission frequency. Solving for the emission frequency shows that at every $\lambda_{th}/2$ of target displacement, where λ_{th} is the emission wavelength without feedback, corresponding to a full 2π phase shift of the round trip.

In practice, the laser output power can be measured using the internal monitor photodiode. The laser output power is related to the emission frequency with feedback and can be written as [11],

$$P = \eta\left(I_{op} + \frac{\kappa_{ext}qV_{act}}{LT_s a\Gamma}\cos(2\pi\nu\tau_{ext}) - I_{th}\right) \ ,$$ (3)

where,

q	elementary charge of the electron,
V_{act}	active volume of the laser cavity,
T_s	spontaneous recombination rate,
a	proportionality constant used in the linearised dependence of the threshold gain, g_{th}, as a function of carrier density, n, in the laser diode depending on the threshold gain carrier density characteristics,
Γ	mode confinement factor,
L	length of laser diode cavity,
I_{op}	operating current of the laser diode,
I_{th}	laser diode threshold current without feedback,

Another quantity that is affected by self-mixing other than the laser optical power is the laser junction voltage V [6]. By considering that r_{2s} and r_{ext} are real, assuming $r_{ext} \ll r_{2s}$ in the first order approximation, the change in laser junction

voltage V can be related to the coupling coefficient of the external cavity and therefore to the level of feedback and the location of the target. Under these assumptions the change in junction voltage can be expressed as:

$$\Delta V = -\frac{4kTn_1\kappa_{ext}}{g_1 q n_0 \tau_L}\cos(2\pi v \tau_{ext}) \qquad (4)$$

where,

n_0	carrier density under steady state condition
n_1	small change in carrier density due to feedback
g_1	change in gain of the laser due to feedback
k	Boltzmann's constant
T	temperature of the laser cavity

It is important to note that according to the eqn (3), output power varies proportionally with the change in target location while eqn (4) exhibits an inverse relationship. This means that an increase in laser power coincides with a decrease in laser junction voltage – the two quantities are out of phase.

3. APPLICATION TO DISPLACEMENT AND RANGE FINDING

Equation (3) shows that the power of the laser exhibits a sinusoidal relationship with the target distance, L_{ext}, since the round-trip propagation time of the external cavity, τ_{ext}, is proportional to the length of the external cavity. Periodic changes in the power, which also correspond to mode hops in the external cavity laser, occur at the frequency $v \tau_{ext}$ for every $\lambda_{th}/2$ of the target displacement along with a 2π shift in the round trip phase. This means that the target displacement can be calculated by counting the number of peaks between the initial and the final position of the target where the spacing between the two consecutives peaks corresponds to the distance of $\lambda_{th}/2$.

Unlike displacements measurements, the target is stationary for the range finding system. An alternative method has to be implemented to introduce the external cavity mode hops. The same phenomenon is observed by modulating the laser driving current. As the optical frequency changes with laser current, a number of distinct resonant modes are developed in the cavity the frequency of the laser being forced to closest one of these modes. Again, the frequency of each mode depends on the round trip phase shift of the external cavity. Therefore, the frequency spacing between these modes is proportional to the target distance.

The change in the frequency of the light can be obtained by modulating the current of the laser with a triangle wave which consequently changes the natural emission frequency of the laser in a time-linear fashion. We need to introduce an additional parameter to indicate the amount by which the optical frequency changes with the change in injected current. This parameter is known as the frequency modulation coefficient, Ω, and is expressed in GHz/mA. We can then use this parameter to solve for the emission frequency and hence the output power.

The resulting output power waveform of the laser is a triangle wave superimposed with small variations corresponding to the different resonant modes occurring in the external cavity. This is shown in fig. 3 for the simulated and experimental results for the self-mixing type range finder. By differentiating the power waveform, the small variations are transformed into a series of sharp peaks.
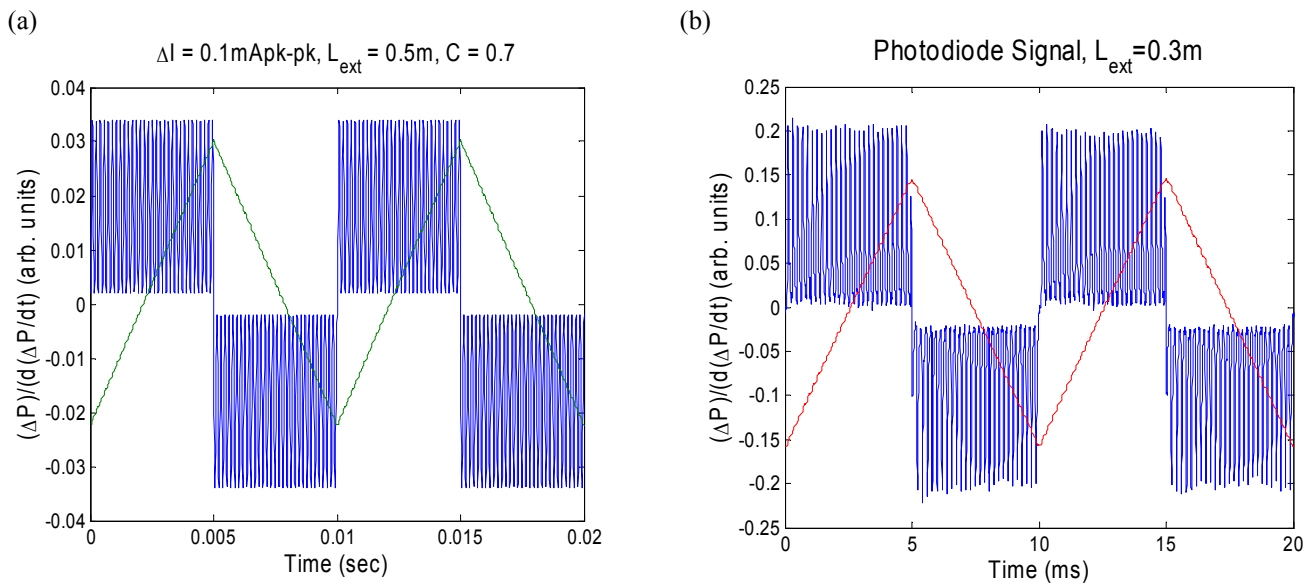
(a)　　　　　　　　　　　　　　　　　　　　　　(b)

Figure 3: Simulated (a) and experimental (b) power fluctuation curves for frequency modulated laser with feedback

The peaks correspond to the resonant modes in the cavity and the frequency spacing between the modes is proportional to the average spacing between the peaks in time. The distance to the target can then be finally calculated as [11],

$$L_{ext} = \frac{c}{4i_{pk-pk}\Omega f_m P_{avg}}$$

(5)

where,

i_{pk-pk}	peak to peak amplitude of the modulating current (mA)
f_m	modulating frequency
p_{avg}	average spacing between peaks (sec)

The spacing between the peaks can be deduced by counting the number of peaks in the differentiated waveform. The conventional method used by other researchers [1, 5], is to set a threshold level at which the number of peaks over this level can be counted. This number is then divided by the time between the first and last peak to give the average peak spacing. There are a number of problems associated with this method and they have been discussed in earlier studies [5, 13, 14]. It is known that the amplitude of the peaks shown in fig. 3 is not constant throughout the measurement range. The noise also will also increase with target distance. Thermal effects in the laser diode and laser thermal transient response contribute further to non-uniform height of the peaks through the differentiated waveform. Therefore, this scheme suffers from the inherent limitations of setting a perfect threshold in the presence of noise and a low quality response.

An alternative method of acquiring the average peak spacing has been described in previous papers [15-17]. This method detects the average frequency of the peak occurrence in the frequency domain. The Fast Fourier Transform (FFT) of the differentiated waveform gives the frequency spectrum of the signal. Neglecting the peak due to the modulation frequency of the laser the strongest peak in the spectrum corresponds to the frequency of the peaks in the differentiated waveform. In this method there is no need to set a threshold so signals with peaks of various heights can be used. This makes the FFT method more robust than the peak spacing methods for low signal levels and in the presence of noise.

4. EXPERIMENTAL SETUP

For this experiment, a single mode oxide confined VCSEL (Avalon Photonics AP-A53-0101-1601) with an internal monitoring photodiode was used. The laser has a threshold current of 3 mA and a peak wavelength of 850 nm.

Figure 4 shows the setup of the displacement and ranging systems. The VCSEL is placed in a mount which is fixed on an optical rail. A lens is used to collimate the laser beam. The target chosen for this experiment is a circular piece of sandblasted aluminum which behaves closely to a diffused reflector, resulting in week feedback. It is mounted on a kinematic platform integrated with a single axis translation stage incorporated with a piezo-electric actuator (Thorlabs PE4) to provide fine translation along the optical axis of the laser beam and minor tilt adjustments. The piezo actuator is driven by a Thorlabs single channel Piezo controller (MDT694A).
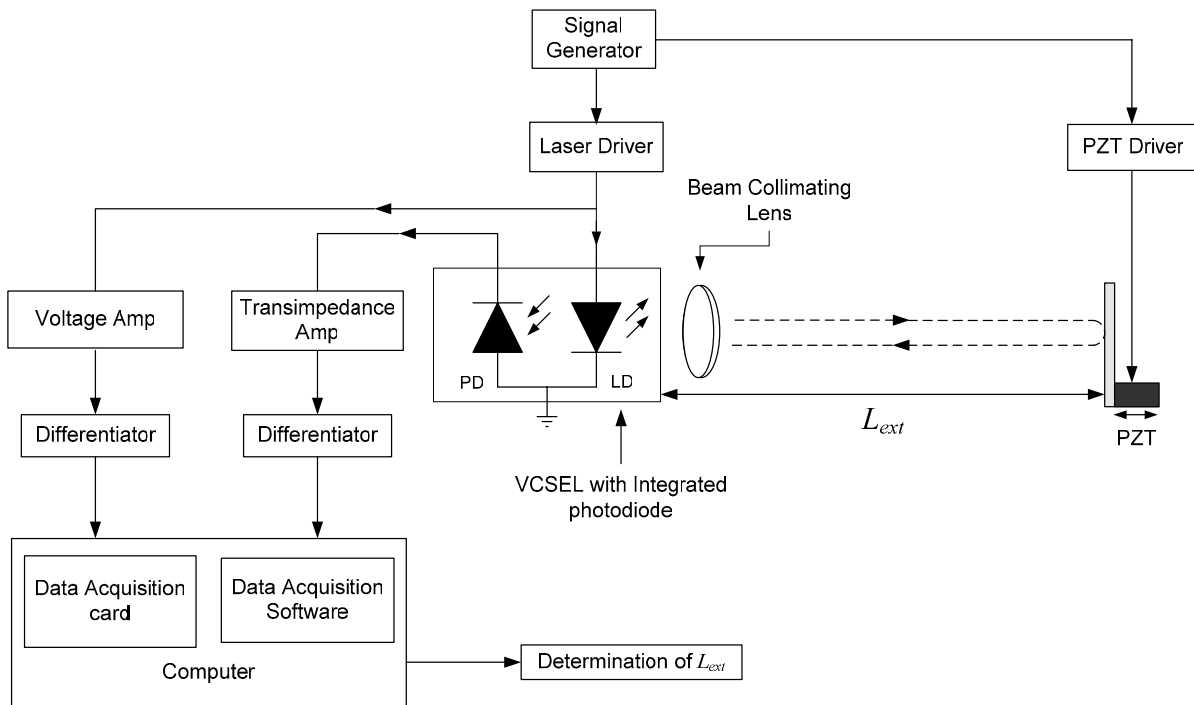

Figure 4: Block Diagram of Experimental Setup

The DC bias current of the laser was set at 4 mA by the laser driver circuit. For displacement measurements, the VCSEL remains DC biased. A signal generator (Agilent 33220A) was used to modulate the position of the target with the integrated piezo actuator.

For measuring the distance, the target remains stationary (i.e. not modulated) while the signal generator was used to generate the desired modulation waveform of 1 V peak to peak at a frequency of 100 Hz. This voltage is then converted into a current by the laser driver circuit to modulate the laser with a corresponding current fluctuation of 0.1 mA peak to peak.

The light from the laser is being reflected back into the laser cavity by the external reflector causing power-fluctuations due to self-mixing in both situations where there is a change in target distance (i.e. displacements) or due to the modulation of laser current. These power fluctuations are monitored using both current and voltage schemes. For the conventional current detection scheme, the internal photodiode is used to detect power fluctuations in the light and generate a proportional photocurrent which is converted into a voltage using a transimpedance amplifier. For the voltage scheme, voltage across the laser is directly tapped and amplified by a voltage amplifier. The ac junction voltage consists of voltage fluctuation which is proportional to power fluctuations in the light. Both current and voltage signals are sent

to the differentiator circuit. The output of the differentiator produces a waveform with sharp peaks and is connected to a National Instruments 12-bit data acquisition card in the PC.

LabView was then used to perform additional signal processing on the differentiated power signal to improve the accuracy and stability of the range finding system. A single 100 Hz period of the input signal was sampled at 60 kHz and passed through to a FFT algorithm to produce a power spectrum array. Eight consecutive power spectra were summed and averaged to reduce the effects of random noise. The major peak power and frequency of the averaged spectrum were then determined, with frequencies below 1 kHz excluded, (though array manipulation), to avoid domination by the 100 Hz modulation signal. One hundred of these processed spectra, major peak frequencies and powers were then recorded to disk for further analysis in Matlab.

5. RESULTS AND ANALYSIS

The system described in the previous section was first used to measure target displacement. A sine wave of 1 V (peak-peak value) is supplied to the piezo actuator controller to induce small oscillating movement of approximately 4 μm in length along the optical axis of the laser beam. Figure 5 shows the photocurrent and junction voltage waveforms each containing 11 peaks corresponding to 10 half wavelength spacing. This corresponds to displacement of 4.25 μm giving us a 0.25 μm resolution. As expected from the model the voltage signal produces peaks corresponding to those of photo current signal but with π phase shift. However, the number of peaks and the spacing between them are identical in both signals. Conventional technique of direction discrimination from photocurrent signal is based on detecting the slopes of the peaks. The voltage signal has a clear advantage over current signal as the direction can be obtained from the polarity of the differentiated voltage waveform. This suggests that by setting appropriate threshold levels, displacement direction can be easily resolved from the polarity of the voltage signal.
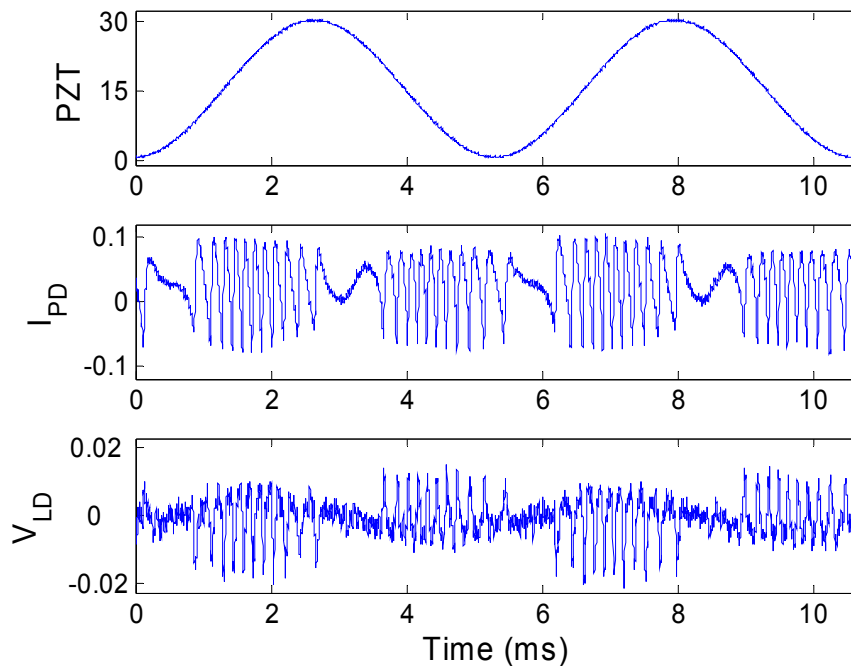

Figure 5 Measure target displacements at L_{ext} =0.2

In range finding mode, the measurements were carried out from 0.2 to 0.7 m at 0.05 m intervals. Theoretically, the maximum measurable distance is ultimately limited to half the coherence length of the laser due to the finite spectral linewidth of the VCSEL spectrum. Another restriction is related to the amount of feedback required for sufficient signal to noise ratio and is related to the target reflectivity and the aperture of the receiver lens. Which of the two limiting factors will be reached first clearly depends on the VCSEL and the optical design of the system.
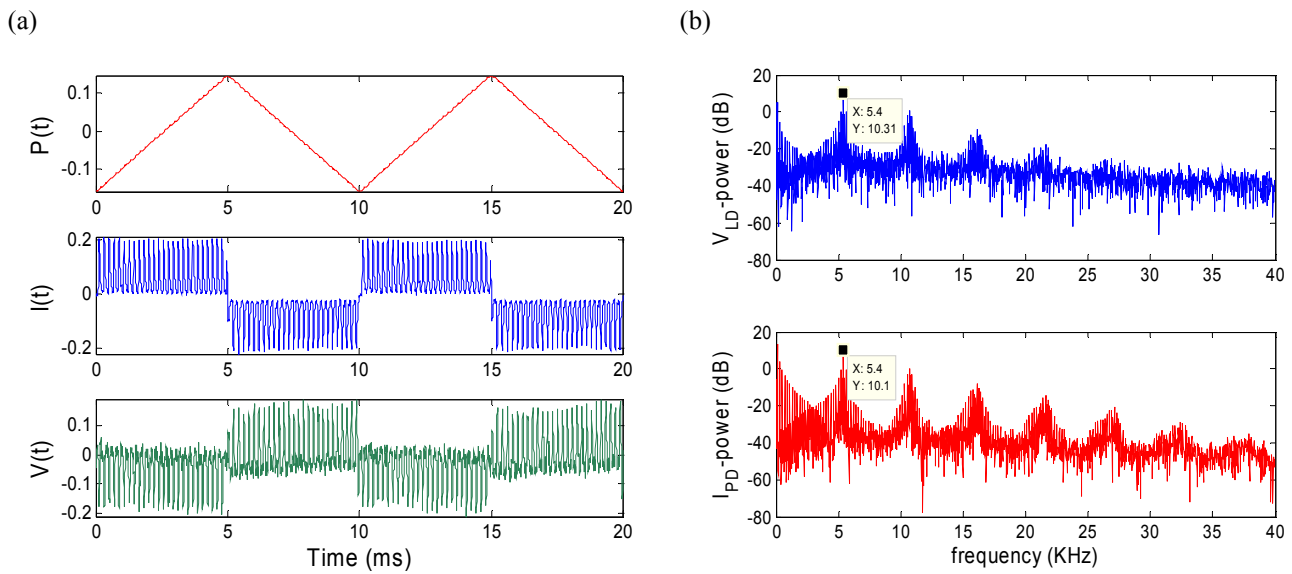
Figure 6: Experimental Time domain signal (a) and its frequency spectrum (b) at target distance (L_{ext}) of 0.3 m method.

From fig. 6, it is clear that both the current and the voltage waveforms contain the same frequency components even though the voltage waveform in time domain appears very different and much noisier. The noise translates to an increase of 10 dB in noise floor of the voltage signal when compared to the photodiode signal. This suggests that the maximum measurable distance with junction voltage will be shorter than using photodiode due to a higher noise floor of around 10 dB.

Nevertheless, the distances measured using both techniques show good agreement with the actual ones as fig. 7(a) shows. Even the error trend of both schemes follows each other very closely as shown in fig. 7(b).
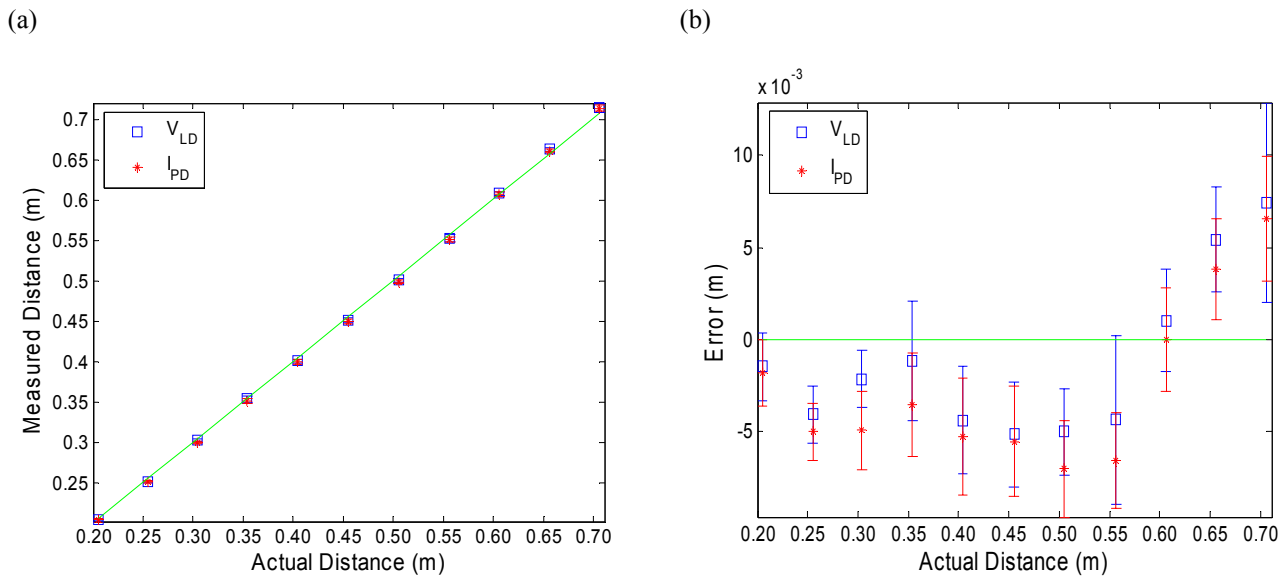

Figure 7: **a**) shows the actual versus measured distance and **b**) shows the corresponding error of the system for each detection method

The accuracy and precision of the two measurements systems is quite similar. The accuracy and deviation of the photodiode and voltage measurements from the actual distance follow the same pattern with a small consistent offset between the distances measured by each system. The precision of the systems was also similar as indicated by the similarly sized error bars in most cases overlapping by greater than 75 %. This shows that the photodiode and voltage measurement schemes provide almost identical performance in monitoring self-mixing within a laser diode to measure distance.

6. CONCLUSIONS

In this study, we have demonstrated a new voltage detection technique for a VCSEL based range finder displacement sensor. We have compared the acquired voltage signal with the conventional photodiode signal over the range of 0.2 to 0.7 m in both displacement and range finding operating regimes. Resulting waveforms extracted after signal processing from both implementations contained the same features even though the voltage sensing scheme exhibited comparatively lower signal to noise ratio. We have demonstrated that the performance of voltage sensing in a self-mixing measurement system is almost identical to that of conventional photocurrent sensing scheme in both displacement and distance measurement modes. Therefore, while the accuracy and precision of the two measurement schemes are comparable the simplicity of implementation of the voltage sensing scheme gives it clear practical advantage over the conventional photocurrent sensing scheme.

REFERENCES

[1]   G. Beheim and K. Fritsch, "Range finding using frequency-modulated laser diode," *Appl. Opt.*, vol. 25, pp. 1439-1442, 1986.
[2]   S. Donati, L. Falzoni, and S. Merlo, "A PC-Interfaced, Compact Laser-Diode Feedback Interferometer for Displacement Measurements," *IEEE Trans. Instrum. Meas.*, vol. 45, pp. 942-947, 1996.
[3]   T. Bosch, N. Servagent, F. Gouaux, and G. Mourat, "The self-mixing interference inside a laser diode: application to displacement, velocity and distance measurement," *Proc. SPIE*, vol. 3478, pp. 98-108, 1998.
[4]   S. Merlo and S. Donati, "Reconstruction of Displacement Waveforms with a Single-Channel Laser-Diode Feedback Interferometer," *IEEE J. Quantum Electron.*, vol. 33, pp. 527-531, 1997.
[5]   F. Gouaux, N. Servagent, and T. Bosch, "Absolute distance measurement with an optical feedback interferometer," *Appl. Opt.*, vol. 37, pp. 6684-6689, 1998.
[6]   R. Justaitis, N. P. Rea, and T. Wilson, "Semiconductor laser confocal microscopy," *App. Opt.*, vol. 33, pp. 578-584, 1994.
[7]   P. J. Rodrigo, M. Lim, and C. Saloma, "Optical-feedback semiconductor laser Michelson interferometer for displacement measurements with directional discrimination," *Appl. Opt.*, vol. 40, pp. 506-513, 2001.
[8]   K. Petermann, *Laser diode modulation and noise*, 1991 ed: Dordrecht ; Boston: Kluwer Academic Publishers ; Tokyo : KTK Scientific Publishers,, 1991.
[9]   N. Servagent, G. Mourat, F. Gouaux, and T. Bosch, "Analysis of some intrinsic limitations of a laser range finder using the self-mixing interference," *Proc. SPIE*, vol. 3479, pp. 76-83, 1998.
[10]   M. Wang and G. Lai, "Self-mixing microscopic interferometer for the measurement of microprofile," *Opt. Commun.*, vol. 238, pp. 237-244, 2004.
[11]   E. Gagnon and J. F. Rivest, "Laser range imaging using the self-mixing effect in a laser diode," *IEEE Trans. Instrum. Meas.*, vol. 48, pp. 693-699, 1999.
[12]   M. Wang, T. Sato, G. Lai, and S. Shinohara, "Self-mixing interferometry for distance and displacement measurement by Fourier transform method," *Proc. SPIE*, vol. 3945, pp. 193-200, 2000.
[13]   F. Gouaux, N. Servagent, and T. Bosch, "Influence of the Thermal Effects on the Accuracy of a Backscatter-Modulated Laser Diode Range Finder," presented at Proceedings of the 3rd International Congress on Optoelectronics, Optical Sensors and Measuring Techniques, Erfurt, Germany, 1998.
[14]   T. Bosch, S. Pavageau, D. D'Alessandro, N. Servagent, V. Annovazi-Lodi, and S. Donati, "A low cost, optical feedback range-finder with chirp-control," presented at 18th IEEE Instrumentation and Measurement of Informatics -Rediscovering Measurement in the Age of Informatics, Budapest, Hungary, 2001.
[15]   K. Bertling, J. R. Tucker, and A. D. Rakic, "Optimum injection current waveform for a laser rangefinder based on the self-mixing effect," *Proc. SPIE*, vol. 5277, pp. 334-345, 2003.

[16]   J. R. Tucker, Y. L. Leng, and A. D. Rakic, "Laser range finding using the self-mixing effect in a vertical-cavity surface-emitting laser," Conference on Optoelectronic and Microelectronic Materials and Devices, 583-583, IEEE, Sydney, Australia, 2002.

[17]   M. Wang, "Fourier transform method for self-mixing interference signal analysis," *Optics & Laser Technology*, vol. 33, pp. 409-416, 2001.